 doi:10.20944/preprints201806.0019.v1

Facile Synthesis of Porous Pt-Cu Alloy with Enhanced Catalytic Activity

Xiang Li, Jiao-Jiao Su, Ying-Xin Li, Shi-zhang Qiao, Hui Liu, Xi-Wen Du

Institute of New-Energy Materials, School of Materials and Engineering, Tianjin University, Tianjin 300072, People's Republic of China

Abstract

Cost-efficient catalyst for hydrogen evolution reaction (HER) and methanol oxidization reaction (MOR) is of great importance for industrial application. The alloying of platinum with cheap transition metal offers a great opportunity to reduce cost and enhance the electro-catalytic performance. Herein, we report a simple and green route to synthesize porous Pt-Cu catalysts, where Pt-Cu solid particles were first produced by using cuprous chloride (CuCl) nanoparticles as the template, followed by a dealloying treatment to obtain final porous product. The porous alloy nanoparticles show higher catalytic activity and superior stability for HER and methanol oxidation reaction, which is beneficial from the porous structure and synergetic effect between Pt and Cu.

Keyword Pt-Cu, porous, electrocatalyst, HER, synergetic effect

Introduction

Hydrogen (H_2) is considered as an ideal energy carrier and one of the most efficient fuels.[1-2] The electrolysis of water via hydrogen evolution reaction (HER) has been proven as an efficient strategy for hydrogen production, where platinum (Pt) is usually employed as a highly effective catalyst of HER. However, the high cost of Pt catalyst limits it large-scale commercialization.[3-4] In addition, Pt catalysts are usually unstable under working conditions, resulting in deactivated facets and the reduction of catalytic activities.[5-6]

In this regard, Pt-based catalyst with different structure and composition was studied for optimizing their catalytic properties.[7-10] Among them, Pt-based bimetallic alloy catalysts with less expensive transition metals such as Pt-Ni,[11] Pt-Fe,[12] Pt-Cu,[7-8] and Pt-Co[9-10] have been proposed as promising alternatives. The alloying of Pt with some secondary metals offers a great opportunity to enhance the electro-catalytic performance due to the changes in the geometric and electronic

Preprints (www.preprints.org) | NOT PEER-REVIEWED | Posted: 1 June 2018 doi:10.20944/preprints201806.0019.v1

structures of Pt.[13-14] On the other hand, the catalytic performance also depends on the surface area of catalysts, which could be improved by generating hollow or porous structures.[15] For instance, Pt_3Ni nanocrystals with a porous feature were demonstrated very efficient for oxygen reduction reaction.[11, 16] Pt-Cu nanoframes are active catalysts for formic acid and methanol oxidation,[17] and mesoporous Pt film is efficient and durable for methanol oxidation reaction (MOR).[18]

Herein we report a facile method to synthesize porous Pt-Cu nanoparticles using cuprous chloride seeds as sacrificial templates and creating porous cavities through the dealloying treatment by immersing in nitric acid to form porous structure. The porous Pt-Cu alloy nanoparticles exhibit superior catalytic activity for HER and MOR, as well as a much higher anti-CO poisoning performance, due to the possible synergetic effect of the two metallic components. Our work offers a promising method for various alloy catalysts with controllable composition and large surface area.

Experimental Methods

Materials. Commercial platinum/carbon (Pt/C) (Pt loading: 20 wt%, Pt on carbon black) was purchased from Alfa Aesar. Cuprous chloride (CuCl, powder, 97.0%), Potassium hexachloroplatinate (IV) (K_2PtCl_6), potassium chloride (KCl, 99.5%), potassium hydroxide (KOH, 85.0%), nafion perfluorinated resin solution, methanol (CH3OH, 99.5%) were purchased from Tianjin Chemical Reagent (Tianjin, China).

Synthesis of CuCl NCs. To obtain uniform CuCl NCs, 0.1g CuCl micropowder was first dissolved in saturated KCl, giving an $HCuCl_2$ solution. Then the solution was added lots of pure water. As a result, the reverse reaction (i. e. CuCl precipitation) could proceed at very high rates, leading to uniform CuCl nanocubes (NCs) formed via quick and homogenous nucleation and growth[19].

Synthesis of porous Pt-Cu NPs. Porous Pt-Cu NPs are synthesized by mixing 10 mL of 1 mM K_2PtCl_6, and 10 mL of as-prepared uniform CuCl NCs, and then the mixture is stirred at room

Preprints (www.preprints.org) | NOT PEER-REVIEWED | Posted: 1 June 2018 doi:10.20944/preprints201806.0019.v1

temperature until the solution color changes from milk white to black, then Pt-Cu NPs are obtained. The synthesized Pt-Cu NPs was immersed into concentrated nitric acid (HNO_3) solution for 30 h. The final product was collected by centrifugation at 12000 rpm for 20 min, followed by three consecutive washing/centrifugation cycles with water, and then stored for further characterization. To avoid particle aggregation, the alloyed Pt-Cu nanoparticles were supported on carbon nano tube (CNT). The final product contains 20 wt% Pt element.

Characterization. The particle size and morphology were investigated using an FEI Technai G^2 F20 transmission electron microscope (TEM) equipped with a field-emission gun and an energy dispersive spectrum (EDS) unit. X-ray diffraction (XRD) was recorded on a Bruker D^8 ADVANCE diffractometer equipped with Cu Kαradiation. X-ray photoelectron spectroscopy (XPS) analyses were performed using a PHI Quantum 2000 scanning ESCA Microprobe spectrometer. The inductively coupled plasma optical emission spectrometry (ICP-OES) analysis was conducted using a Thermo Scientific iCAP6300 (Thermo Fisher Scientific, US). The specific surface area was evaluated by the Brunauer-Emmett-Teller (BET) method, which was carried out at -196°C on Microporous instrument Tristar 3000.

Electrochemical investigations. Electrochemical measurements were performed using a standard three-electrode glass cell (CHI 660D). The electrolyte cell was composed of three electrodes: a glassy carbon with an area of 0.07 cm^2 as the working electrode, a saturated calomel electrode (SCE) as the reference electrode, and graphite plate was used as the counter electrode. The measurements were conducted in solution.

One milligram of Pt-Cu NPs were dispersed in a mixture containing 0.5 mL of isopropanol, 0.5 mL of deionized water and 10 μL of Nafion (0.5 wt %) ultrasonicating for approximately 0.5 h to

Preprints (www.preprints.org) | NOT PEER-REVIEWED | Posted: 1 June 2018 doi:10.20944/preprints201806.0019.v1

form a 1 mg mL−1 catalyst ink. The catalyst ink (3 μL) was deposited on the glassy carbon working electrode (diameter = 3 mm) that was polished prior to catalyst deposition by 0.3 and 0.05 mm alumina powder. Then the working electrode was dried in air. The HER experiments with chronoamperometric (CV) and LSV measurements of Pt-Cu/CNT、Pt/C catalysts were conducted in N_2 saturated 0.5 M H_2SO_4.

Results and discussion

The Pt-Cu nanoparticles (NPs) were prepared by using cuprous chloride seeds as sacrificial templates. CuCl was proven to be an ideal template for the preparation of new structures via self-disproportionated reaction in our previous work.[19] Meanwhile, the standard reduction potential of Cu(II)/Cu(I) (0.153 V vs. SHE) is much lower than that of the $PtCl_6^{2-}$/Pt pair (0.735V vs. SHE). Thereafter, CuCl was introduced to prepare Pt-Cu alloy. Firstly, the disproportionation reaction of CuCl takes place as the pH value ranges from 2.4 to 5.0,[19] giving rise to Cu^{2+} and Cu atoms,

$$2CuCl = Cu_{atom} + Cu^{2+} + 2Cl^- \quad (1)$$

Meanwhile, $PtCl_6^{2-}$ is reduced by CuCl to Pt atoms,

$$4CuCl + PtCl_6^{2-} = Pt_{atom} + 4Cu^{2+} + 10Cl^- \quad (2)$$

The produced Cu and Pt atoms would form Pt-Cu alloy, just like the case via coreduction method.[20] as shown in Figure S1, the PtCu alloy sample before dealloying contains fine grains with high crystallinity. The synthesized Pt-Cu NPs were then etched by concentrated nitric acid (HNO_3) solution for 30 h, and part of the Cu atoms were removed and the ratio of Pt:Cu changed from 1:1 to 4:1 as demonstrated from the inductively coupled plasma mass spectrometry (ICP-MS) results (Table S1). The schematic diagram is shown in Figure S2. Furthermore, the composition of Pt-Cu alloy could be tuned through the adjusting the concentration of the Pt precursor (Figure S3).

After dealloying, porous Pt-Cu NPs were obtained with the diameter range from 50 to 100 nm (Figure 1a). The inset energy dispersive spectrum (EDS) in Figure 1a confirmed that both Pt and Cu elements were present in the nanoparticles. The EDS mapping image taken from the marked regions in Figure 1a reveal a homogeneous distribution of Pt and Cu elements throughout the particle (Figure 1b and c). The porous structures of Pt–Cu can be clearly observed in the high

Preprints (www.preprints.org) | NOT PEER-REVIEWED | Posted: 1 June 2018 doi:10.20944/preprints201806.0019.v1

resolution transmission electron microscope (HRTEM) image (Figure 1d), and the pore size is about 1.5 nm. The crystalline structure of the porous Pt-Cu NPs was analyzed by X-ray diffraction (XRD). The pattern of the as-synthesized nanoparticles shows a typical face-centered-cubic (fcc) structure of the Pt-Cu alloys, and the leaching of Cu atoms in dealloying Pt-Cu alloy leads to an obvious shift to a smaller diffraction angle due to the lower content of Cu.. Furthermore, there is no Cu peak found in the pattern, demonstrating the formation of Pt-Cu alloys.

The X-ray photoelectron spectroscopy (XPS) analysis was further used to investigate the electronic state of Pt-Cu before and after dealloying treatment (Figure 1f). Two peaks at 71.55 eV and 74.85 eV which corresponds to Pt $4f_{7/2}$ and Pt $4f_{5/2}$ are found for Pt-Cu before dealloying, the two peaks shifted to lower energy (71.06 and 74.36 eV for Pt $4f_{7/2}$ and Pt $4f_{5/2}$, respectively) after dealloying. Such shifts in binding energy suggest the electron transfer from Cu to Pt become weak. The shift in energy states of Pt may improve the catalytic activity of Pt-Cu NPs for HER.[21]

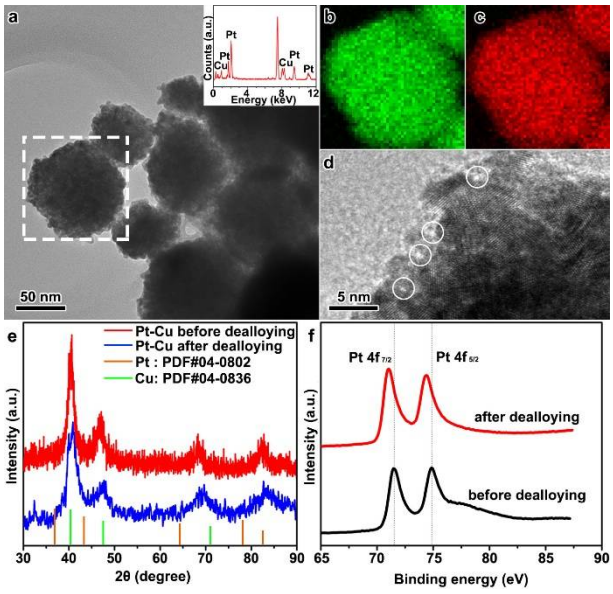

Figure 1 Characterizations of the porous Pt-Cu NPs. (a) TEM image, the inset image is EDS spectrum, (b) and (c) EDS elemental mapping, (d) HRTEM image, (e) XRD spectra of Pt-Cu alloy before and after dealloying, (f) XPS spectra of Pt 4f of Pt-Cu alloy before and after dealloying.

Preprints (www.preprints.org) | NOT PEER-REVIEWED | Posted: 1 June 2018 doi:10.20944/preprints201806.0019.v1

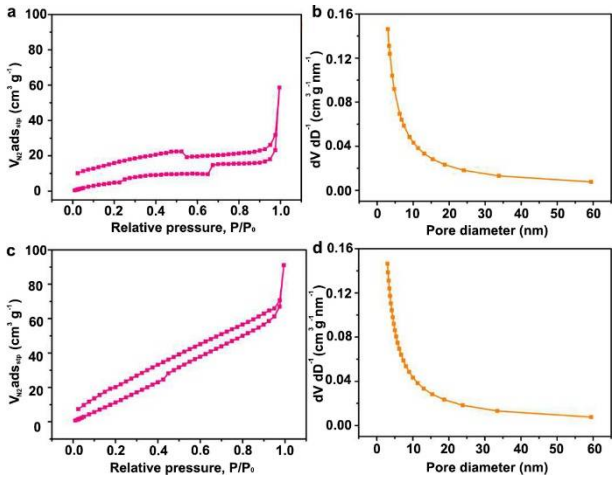

Figure 2 N_2 adsorption-desorption isotherms and pore-size for porous Pt-Cu NPs before dealloying (a and b) and after dealloying (c and d).

Brunauer–Emmett–Teller (BET) surface area of Pt-Cu NPs (Figure 2) were measured by N2 adsorption–desorption analysis. Before dealloying, the Pt-Cu NPs present a surface area of 30.886 $m^2\ g^{-1}$ and a pore volume of 0.031 $cm^3\ g^{-1}$, after dealloying, the surface area and pore volume increase to 92.698 $m^2\ g^{-1}$ and 0.106 $cm^3\ g^{-1}$, respectively. The higher surface area and pore volume are ascribed to the formation of pores in Pt-Cu NPs after dealloying treatment. These results indicate that the dealloying process is favorable for the synthesis of porous Pt-Cu NPs, the large surface area provides many active sites and facilitates fast mass transport for enhancing reaction kinetics, and thus results in better catalytic performance.

Preprints (www.preprints.org) | NOT PEER-REVIEWED | Posted: 1 June 2018 doi:10.20944/preprints201806.0019.v1

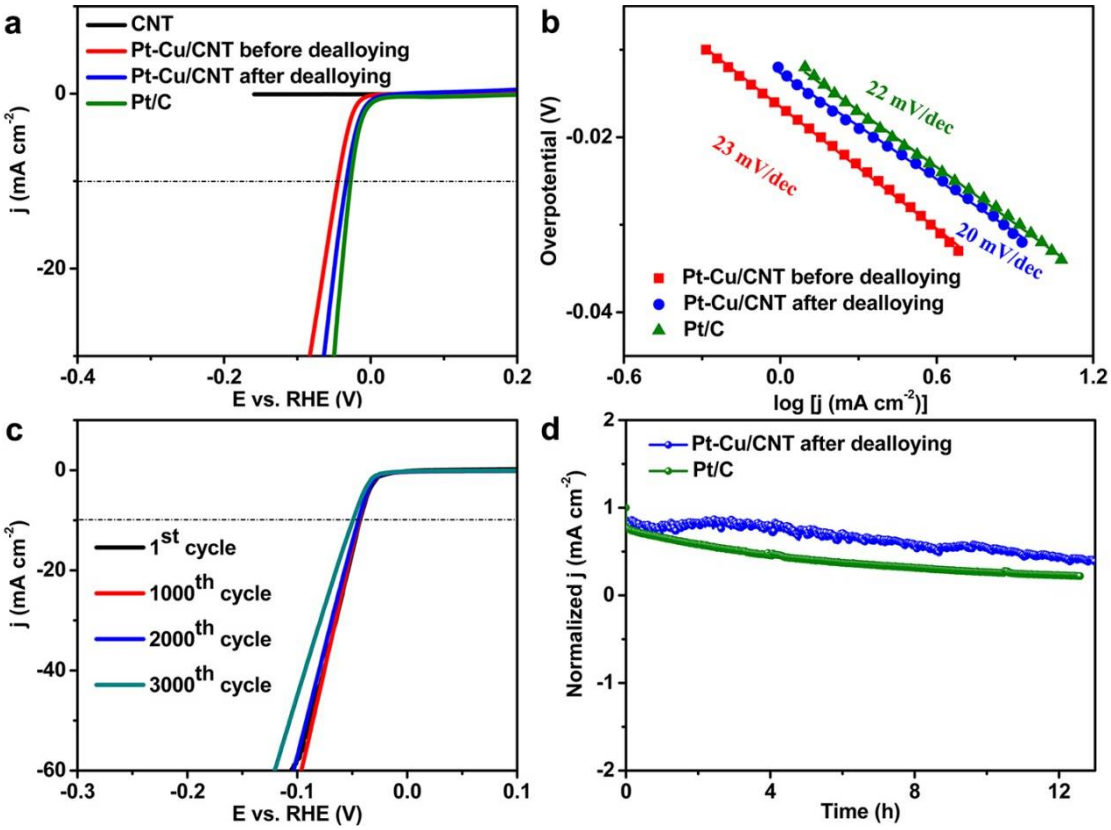

Figure 3 The HER performance of Pt-Cu/CNT and Pt/C. (a) the HER polarization curves, (b) the Tafel plots for CNT, Pt-Cu/CNT bafore and after dealloying, Pt/C (electrolyte: 0.5 M H_2SO_4, scan rate: 5 mV/S); (c) LSV of the Pt-Cu/CNT after dealloying before and after 1000 (2000/3000) cycles in N_2-saturated 0.5 M H_2SO_4; (d) Constant potential polarization curve of the Pt-Cu/CNT and Pt/C after dealloying at -0.04 V vs. RHE in N_2-saturated 0.5 M H_2SO_4.

The activity of porous Pt-Cu catalysts toward HER was evaluated in 0.5 M H_2SO_4 by using a typical three-electrode system with scan rate of 5 mV/s, and the results were shown in Figure 3. For comparison, other catalysts such as carbon nanotubes (CNT), Pt/C were also measured under the same conditions. Figure 3a shows the HER linear sweep voltammetry (LSV) curves of various catalysts on the RHE scale. It is clear that CNT does not exhibit HER activity at all, while the Pt-Cu/CNT after the dealloying treatment shows better electrocatalytic activity, the onset potential (@10 mA cm^{-1}) is positively shifted to -45 mV, similar with that of Pt/C (-33 mV), which should be attributed tothe synergistic effect and the porous structure of Pt-Cu alloy, as well as the improvement of conductivity by the CNT substrate. Figure 3b shows the corresponding tafel plots for Pt-Cu/CNT and Pt/C. The measured tafel slopes for Pt-Cu/CNT before and after dealloying treatment and Pt/C were 23, 20 and 22 mV dec^{-1}, respectively. The porous Pt-Cu/CNT exhibited

Preprints (www.preprints.org) | NOT PEER-REVIEWED | Posted: 1 June 2018 doi:10.20944/preprints201806.0019.v1

the smallest tafel slope of 20 mV dec^{-1}. The long-term durability for the HER in 0.5 M H_2SO_4 were shown in Figure 3c and 3d. Polarization curves for HER before and after 1000 (2000/3000) potential cycles were recorded. No obvious change was observed after 2000 cycles, indicating the significant durability of the porous Pt-Cu/CNT. In addition, the time-dependent current density curve also exhibited favourable durability. Therefore, it is suggested that the porous Pt-Cu/CNT could work as a durable electrocatalyst for practical applications.

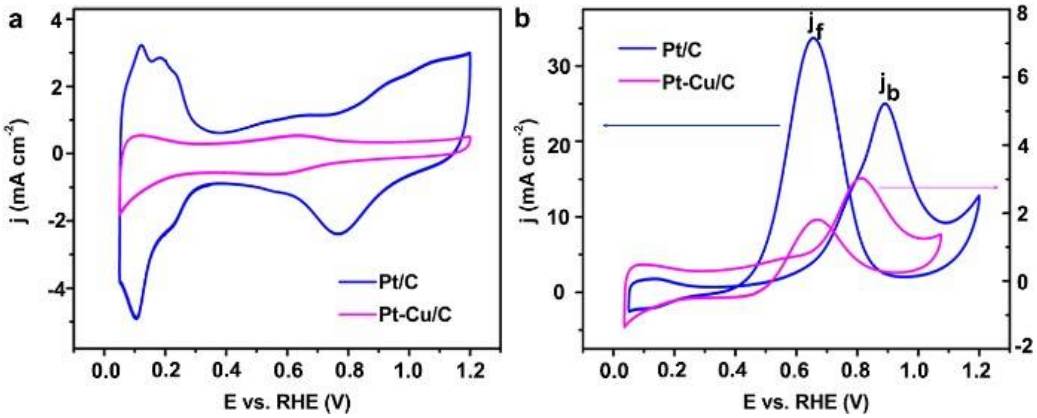

Figure 4 (a) Comparison of the CVs of the porous Pt-Cu/C NPs and Pt/C in an aqueous solution containing 0.5 M H_2SO_4. (b) CVs for methanol oxidation reactions catalyzed with the porous Pt-Cu/C NPs and Pt/C in an aqueous solution containing 0.5 M H_2SO_4 and 1 M methanol. Scan rate: 50 mV/s.

We also tested the catalytic performance for methanol oxidization reaction (MOR). Pt and its alloys are widely used as effective catalysts for direct methanol fuel cell (DMFC)[22-24], but they usually suffer from serious carbon monoxide (CO) poisoning. Pt-Cu alloys have been proved to be high anti-poisoning to CO[22-23]. In 0.5 M H_2SO_4, a pair of peaks at around 0.27 V was found for Pt/C, such peaks are attributed to the hydrogen adsorption–desorption of Pt (Figure 4a). For Pt-Cu, the hydrogen adsorption–desorption features are unconspicuous, similar to that of Pt_3Ni nanoctahedra,[25] indicating the surface of Pt-Cu are Cu-rich. During MOR (Figure 4b), the backward peak (J_b) is the indicator for CO stripping and anti-poisoning of CO, obviously, Pt-Cu/C presents more negative peak than Pt/C due to the abundance of Cu on the surface of Pt-Cu alloy. On the other hand, the ratio of forward peak (J_f) and the forward peak (J_b) is 1.68 for Pt-Cu/C, much higher than that of Pt/C (0.74), implying the superior tolerance to CO poisoning of Pt-Cu/C.

The excellent performance of the Pt-Cu alloys should contribute to the several specific features: (1) the porous Pt-Cu possess high surface areas and many active sites, which are favorable for the HER. (2) The synergistic effect between Pt and Cu atoms in the alloy, which is vital for the high

 doi:10.20944/preprints201806.0019.v1

electrocatalytic activities. (3) The anti-corrosion capability of CNT endows the Pt-Cu/CNT excellent electrochemical salability.

In summary, we have developed an economical, environmentally friendly and controllable approach to synthesize porous Pt-Cu NPs. Compared with commercial Pt/C catalysts, the porous Pt-Cu NPs not only reduces Pt consumption, but also exhibit superior catalytic activity, better durability for HER and higher tolerance to poisoning species. The high performance may arise from the possible synergetic effects and the porous structure. This work explores a new way towards porous Pt-Cu catalysts and is expected to expand to other material systems.

Acknowledgements

This work was supported by the National Basic Research Program of China (2014CB931703), the Natural Science Foundation of China (Nos. 51671141, 51571149, and 51471115)

Conflicts of interest

There are no conflicts to declare.

References

1. (a) Fan, Z.; Huang, X.; Tan, C.; Zhang, H., Thin metal nanostructures: synthesis, properties and applications. *Chemical Science* **2015,** *6* (1), 95-111; (b) Dresselhaus, M. S.; Thomas, I. L., Alternative energy technologies. *Nature* **2001,** *414* (6861), 332-337.

2. (a) Debe, M. K., Electrocatalyst approaches and challenges for automotive fuel cells. *Nature* **2012,** *486*, 43; (b) Gasteiger, H. A.; Marković, N. M., Just a Dream—or Future Reality? *Science* **2009,** *324* (5923), 48-49.

3. (a) Lim, B.; Jiang, M.; Camargo, P. H. C.; Cho, E. C.; Tao, J.; Lu, X.; Zhu, Y.; Xia, Y., Pd-Pt Bimetallic Nanodendrites with High Activity for Oxygen Reduction. *Science* **2009,** *324* (5932), 1302-1305; (b) Yu, C.; Holby, E. F.; Yang, R.; Toney, M. F.; Morgan, D.; Strasser, P., Growth Trajectories and Coarsening Mechanisms of Metal Nanoparticle Electrocatalysts. *ChemCatChem* **2012,** *4* (6), 766-770.

4. (a) Fu, S.; Zhu, C.; Shi, Q.; Xia, H.; Dua, D.; Lin, Y., Highly branched PtCu bimetallic alloy nanodendrites with superior electrocatalytic activities for oxygen reduction reactions. *Nanoscale* **2016,** *8* (9), 5076-5081; (b) Chen, Z.; Ye, S.; Wilson, A. R.; Ha, Y.-C.; Wiley, B. J., Optically transparent hydrogen evolution catalysts made from networks of copper-platinum core-shell nanowires. *Energy & Environmental Science* **2014,** *7* (4), 1461-1467; (c) Yu, Y.; Xin, H. L.; Hovden, R.; Wang, D.; Rus, E. D.; Mundy, J. A.; Muller, D. A.; Abruna, H. D., Three-Dimensional Tracking and Visualization of Hundreds of Pt-Co Fuel Cell Nanocatalysts During Electrochemical Aging. *Nano Letters* **2012,** *12* (9), 4417-4423; (d) Yang, T.; Zhu, H.; Wan, M.; Dong, L.; Zhang, M.; Du, M., Highly efficient and durable PtCo alloy nanoparticles encapsulated in carbon nanofibers for electrochemical hydrogen generation. *Chemical Communications* **2016,** *52* (5), 990-993.

5. Chen, C.; Kang, Y.; Huo, Z.; Zhu, Z.; Huang, W.; Xin, H. L.; Snyder, J. D.; Li, D.; Herron, J. A.; Mavrikakis, M.; Chi, M.; More, K. L.; Li, Y.; Markovic, N. M.; Somorjai, G. A.; Yang, P.; Stamenkovic, V. R., Highly Crystalline Multimetallic Nanoframes with Three-Dimensional Electrocatalytic Surfaces. *Science* **2014,** *343* (6177), 1339-1343.

6. Guo, S.; Sun, S., FePt Nanoparticles Assembled on Graphene as Enhanced Catalyst for Oxygen Reduction Reaction. *Journal of the American Chemical Society* **2012,** *134* (5), 2492-2495.

7. (a) Kim, J.; Lee, Y.; Sun, S., Structurally Ordered FePt Nanoparticles and Their Enhanced Catalysis for Oxygen Reduction Reaction. *Journal of the American Chemical Society* **2010,** *132* (14), 4996-+; (b) Zhang, J. L.; Vukmirovic, M. B.; Sasaki, K.; Nilekar, A. U.; Mavrikakis, M.; Adzic, R. R., Mixed-metal Pt monolayer electrocatalysts for enhanced oxygen reduction kinetics. *Journal of the American Chemical Society* **2005,** *127* (36), 12480-12481.

8. Xu, Y.; Zhang, B., Recent advances in porous Pt-based nanostructures: synthesis and electrochemical applications. *Chemical Society Reviews* **2014,** *43* (8), 2439-2450.

9. Huang, X.; Zhu, E.; Chen, Y.; Li, Y.; Chiu, C.-Y.; Xu, Y.; Lin, Z.; Duan, X.; Huang, Y., A Facile Strategy to Pt3Ni Nanocrystals with Highly Porous Features as an Enhanced Oxygen Reduction Reaction Catalyst. *Advanced Materials* **2013,** *25* (21), 2974-2979.

10. Ding, J.; Zhu, X.; Bu, L.; Yao, J.; Guo, J.; Guo, S.; Huang, X., Highly open rhombic dodecahedral PtCu nanoframes. *Chemical Communications* **2015,** *51* (47), 9722-9725.

11. Li, C.; Malgras, V.; Aldalbahi, A.; Yamauchi, Y., Dealloying of Mesoporous PtCu Alloy Film for the Synthesis of Mesoporous Pt Films with High Electrocatalytic Activity. *Chemistry-an Asian Journal* **2015,** *10* (2), 316-320.

12. Liu, H.; Zhou, Y.; Kulinich, S. A.; Li, J.-J.; Han, L.-L.; Qiao, S.-Z.; Du, X.-W., Scalable synthesis of hollow Cu2O nanocubes with unique optical properties via a simple hydrolysis-based approach. *Journal of Materials Chemistry A* **2013,** *1* (2), 302-307.

13. Jia, Y.; Jiang, Y.; Zhang, J.; Zhang, L.; Chen, Q.; Xie, Z.; Zheng, L., Unique Excavated Rhombic Dodecahedral PtCu3 Alloy Nanocrystals Constructed with Ultrathin Nanosheets of High-Energy {110} Facets. *Journal of the American Chemical Society* **2014,** *136* (10), 3748-3751.

14. Yu, X.; Wang, M.; Wang, Z.; Gong, X.; Guo, Z., 3D multi-structural porous NiAg films with nanoarchitecture walls: high catalytic activity and stability for hydrogen evolution reaction. *Electrochimica Acta* **2016,** *211*, 900-910.

15. (a) Liao, Y.; Yu, G.; Zhang, Y.; Guo, T.; Chang, F.; Zhong, C.-J., Composition-Tunable PtCu Alloy Nanowires and Electrocatalytic Synergy for Methanol Oxidation Reaction. *Journal of Physical Chemistry C* **2016,** *120* (19), 10476-10484; (b) Tritsaris, G. A.; Rossmeisl, J., Methanol Oxidation on Model Elemental and Bimetallic Transition Metal Surfaces. *The Journal of Physical Chemistry C* **2012,** *116* (22), 11980-11986; (c) Zhou, Y.-Y.; Liu, C.-H.; Liu, J.; Cai, X.-L.; Lu, Y.; Zhang, H.; Sun, X.-H.; Wang, S.-D., Self-Decoration of PtNi Alloy Nanoparticles on Multiwalled Carbon Nanotubes for Highly Efficient Methanol Electro-Oxidation. *Nano-Micro Letters* **2016,** *8* (4), 371-380.

16. Zhang, J.; Yang, H.; Fang, J.; Zou, S., Synthesis and Oxygen Reduction Activity of Shape-Controlled Pt3Ni Nanopolyhedra. *Nano Letters* **2010,** *10* (2), 638-644.